CHAPTER ONE HUNDRED EIGHTY TWO

MARINE ROUGHENED CYLINDER WAVE FORCE COEFFICIENTS

John H. Nath, Fellow, ASCE*

ABSTRACT

Steel cylinders were submerged on a platform in the South Pass region of the Gulf of Mexico for one year to accumulate biofouling for later laboratory testing to determine wave force transfer coefficients. They were positioned at -55, -140, and -190 feet below the still water surface. Laboratory tests comprised steady tow up to Reynolds number of 7×10^5, and periodic waves up to Reynolds number of 1.6×10^5 and Keulegan-Carpenter number up to 25. The force transfer coefficients for the -55 cylinder were about equal to those for a sand roughened cylinder with relative cylinder roughness, ε/D, of .03, where ε is the height of the equivalent sand roughness size and D is the smooth cylinder diameter. The drag coefficient for very high Keulegan-Carpenter number, or steady tow, is about 1.0 if the effective cylinder diameter is taken into account, for the rougher cylinders.

INTRODUCTION

Most information about force transfer coefficients for cylinders in waves or in steady flow is based on smooth cylinders or cylinders uniformly roughened with glued-on sand. Biofouling, however, can be very irregular, have a much thicker accumulation, and protrude much further into the flow field from the cylinder surface than any sand coated cylinder ever tested.

In order to gather wave force information on cylinders roughened with real marine growths, three 8-5/8 inch diameter steel cyinders were positioned at -55, -140, and -190 feet below the still water surface at a platform positioned in the Gulf of Mexico near the mouth of the Mississippi River at the coordinates 89° 23' East and 28° 50' North. Three cylinders were positioned at each level so that they could be tested after 1, 2, and 3 years' of growth. This paper reports on the results obtained from the 1-year old cylinders.

---

*Professor, Ocean Engineering Program, Dept. of Civil Engineering, Oregon State University, Corvallis, OR 97331.

EQUIPMENT

The cylinders were constructed from 8-5/8 inch diameter steel pipes, 2 feet long. They were split longitudinally so they could be attached to a test beam for the laboratory tests in steady flow and waves (4,5,6), using countersunk, flush-headed machine screws. The test beam was about 10 feet long, mounted horizontally between 2 vertically suspended low-drag support members that were positioned close to the wave flume walls. The support members hung from a tow carriage. The Oregon State Unviersity (OSU) Wave Research Laboratory (WRL), the tow carriage, and the test beam are further described in (4,5,6).

The half cylinders were mounted to strain gage force dynamometers so that the total horizontal and vertical forces could be measured on the 2-foot long test section. They were carefully calibrated in all directions before and after each test with the test beam submerged. The calibration constants were linear and varied by less than 2% between the calibrations prior to the tests and those after the tests. The water surface fluctuation was measured directly above the beam. A current meter was positioned 2 cylinder diameters above the cylinder surface, but the measurements therefrom have not been used in the analysis because of the modification to the rotating flow from the presence of the cylinder.

Two dummy cylinders (each were split) were attached to the test beam to provide a continuous cylindrical surface. They were roughened artificially with glued-on sand, barnacles, corks and fuzzy material to provide a roughness about equal to that of the center test surface. The position of the test section relative to the water surface and wave flume floor is shown in Fig. 1. There was a space of less than 1/8 inch between the test section and the dummy section that did not influence the results, as proved in other testing (6).

Data were recorded digitally on a PDP-11 minicomputer. For reliability there were 2 channels for horizontal force, 2 for vertical force, 1 each for the horizontal and vertical current measurement and 1 for the water surface profile.

Photographs of the cylinders were made by personnel at the ocean platform prior to mounting them in shipping containers of sea water. They were shipped quickly by air freight to OSU, where they arrived with almost all of the organisms still alive. At OSU they were photographed, aerated, and removed from their mounting core prior to placement under water (fresh water) on the test beam. A photograph of the cylinder from -55 feet is shown in Fig. 2.

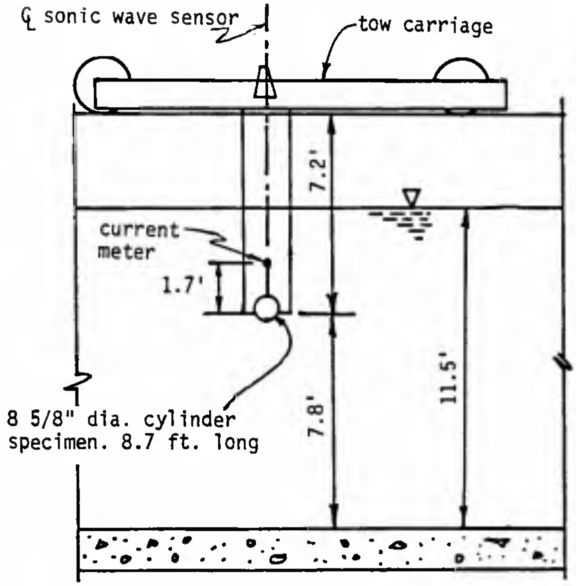

Fig. 1 Horizontal cylinder location in the wave flume.

Fig. 2 Cylinder from -55 feet, South Pass platform.

Most of the organisms stayed alive until placed in fresh water, whereupon the cylinders were immediately tested in steady state towing. They soon died in the fresh water, but they generally remained attached to the cylinder for the remainder of the testing. The test results showed that the death of the organisms caused no appreciable change in the force transfer coefficients.

TESTS

There have been earlier tests on smooth and sand roughened cylinders at OSU (5), some results of which will be repeated here for comparison with the marine roughened cylinders. The South Pass cylinders were first towed at speeds from 1 to 10 fps. Then the ends of the carriage test beam were guyed to the WRL walls for tests in periodic and random waves. (The tests in random waves are not reported on herein.) After the wave tests, the cylinders were again towed to see if there was a detectable change in the steady state drag coefficients due to a loss of biofouling from the fresh water and the vigorous action from waves. The cylinders were then dried and the soft (now crisp) organisms were brushed off. The cylinders were tested again in steady tow to see if there was a detectable change in the steady state drag coefficients due to the loss of the soft, flexible organisms. These 3 conditions of the organisms during the tests are termed "live", "after" and "dried" for this report.

The various cylinder roughnesses are given abbreviated designations in this report for ease in referring to them. These designations are summarized in Table 1.

Table 1. Cylinder designators.

Designation	Explanation
SMC	Smooth cylinder
SRC.02	Sand roughened cylinder with ε/D = .023
SRC.03	Sand roughened cylinder with ε/D = .032
SP1-55	South Pass cylinder, 1 year old, -55 ft,
SP1-140	South Pass cylinder, 1 year old, -140 ft,
SP1-190	South Pass cylinder, 1 year old, -190 ft,

ANALYSIS

The steady state tow drag coefficient, C_{ds}, was calculated from

$$C_{ds} = \frac{F}{\frac{1}{2} DL\rho U^2 \delta} \qquad (1)$$

where F is the average force on the test section, D is the smooth cylinder diameter, L is the test section length (2 feet), ρ is the water mass density, U is the steady tow speed (the carriage was timed over a measured distance), and δ is the effective diameter coefficient ($\delta \geqslant 1$). For very rough and irregular growths, and for significant, flexible biofouling, like heavy accumulations of kelp, it is sometimes difficult to define an effective diameter that can be universally accepted. Therefore, for much of the analysis for this work the coefficient, δ was set equal to 1. Much of the data presented here were so calculated, but for some data δ was computed from the circumferential measurements of the cylinders.

The force transfer coefficients were computed with least squares methods using a vector form of the Morison equation that is reviewed in more detail in (5,11). During a test, measurements were made for 4 wave periods, from which 3 complete crest-to-crest waves could be defined. Coefficients were calculated for each of the 3 waves and averaged. These average values are reported herein.

The Morison equation for the force per unit of length, $\vec{F}$, on a horizontal cylinder is then written as

$$\vec{F} = \frac{1}{2} C_d \,\delta D \,\rho\, \vec{q}|q| + C_m \,\pi \,\frac{(\delta D)^2}{4}\, \rho\, \dot{\vec{q}} \qquad (2)$$

where $\vec{q}$ is the velocity vector and $\dot{\vec{q}}$ is the acceleration vector. In the least squares analysis, C_d and C_m are assumed to be constant with time. If δ is assumed to be 1, the increase in diameter due to biofouling is included in C_d and C_m. Where C_d and C_m are so computed, they can be corrected with appropriate manipulations with the δ desired.

It is well known with respect to wave forces on cylinders that are small in diameter compared to the wave lengths that the averaged force transfer coefficients computed from least squares techniques are functions of the Keulegan-Carpenter number and the Reynolds number. They are defined, respectively, as

$$K = \frac{u_\mu T}{D\delta} \tag{3}$$

and
$$R = \frac{u_\mu D\delta}{\nu} \tag{4}$$

where u_μ is the maximum horizontal water speed at the cylinder position, T is the wave period, and ν is the kinematic viscosity.

More recently the particle orbit shape has been found to influence force transfer coefficients for vertical smooth cylinders. The orbit shape is usually quantified with the ratio

$$\Omega = \frac{u_\mu}{w_\mu} \tag{5}$$

where w_μ is the maximum vertical velocity.

For a horizontal cylinder with the axis parallel to the wave crests the vortex shedding characteristics are influenced considerably by Ω. Without the cylinder present the velocity vector rotates, at the position of the center of the cylinder, in a clockwise direction if the progressing wave is travelling from left to right. The vector changes in magnitude with time if the wave is not a linear, deep water wave. Otherwise, the magnitude remains constant and $\Omega = 1$.

For this work $.4 < \Omega < 1.0$, as detailed in ref. (5). However, the wave conditions were such that K and R could not be varied through the full range for <u>each</u> value of Ω. Therefore, the lower values of Ω are usually associated with the higher values of K and R.

Another way to consider the wave forces is through the maximum force coefficient, C_μ, and the phase shift, $\hat{\phi}$. The first is defined as

$$C_\mu = \frac{F_\mu}{\frac{1}{2} DL\rho u_\mu^2 \delta} \tag{6}$$

and the phase shift is (please refer to Fig. 3)

$$\hat{\phi} = \frac{\phi_f}{\phi_a} \tag{7}$$

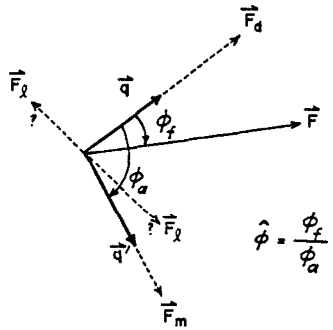

Fig. 3 The velocity vector, $\vec{q}$, drag force, $\vec{F}_d$, acceleration vector, $\vec{q}'$, inertia force, $\vec{F}_m$, "lift" force, $\vec{F}_\ell$, and the phase angles for a wave with the crest parallel to the axis of a submerged horizontal cylinder.

It can be shown (7) that as K gets very large, $C_\mu \to C_{ds}$ in Eq. (6). Where ϕ_f is the instantaneous phase shift (in space) between the velocity vector and the total force vector, and ϕ_a is the phase shift between the velocity vector and the acceleration vector (which = 90° only for deep water small amplitude waves). Note that the "lift" force, $\vec{F}_\ell$, which is orthogonal to the velocity vector, is not included in Eq. (2), so the somewhat random influence from vortex shedding will appear as scatter in both C_d and C_m. However, Eq. (6) should not be influenced quite so much from such effects, so one would expect less scatter in the results for C_μ. On the other hand, $\hat{\phi}$ should be very sensitive to vortex shedding and one would expect considerable scatter in experimental values for $\hat{\phi}$.

There is as much information about the wave force in Eqs. (6) and (7) as in Eq. (2) if one considers $\hat{\phi}$ to be a function of time. Actually, $\hat{\phi}$ is evaluated when F is F_μ. An advantage for Eqs. (6) and (7) is that they conceivably can be based on measurements only. There is no theory involved if $\vec{q}$ is measured in some way. In this paper $\vec{q}$ is based on the water surface profile and Dean's stream function wave theory. For vertical cylinders it is easier to base Eq. (6) on pure measurements. It also turned out that there was much less scatter in the C_μ plots than for C_d and C_m. In this case there is more scatter in $\hat{\phi}$ because of its sensitivity to vortex shedding. Another advantage to Eq. (6) is that u need not be measured right at the cylinder, but can be any distance away, at the same depth. But measurement of the water surface profile, $\eta(t)$, or thoery, must be used to be able to evaluate $\hat{\phi}$ Herein the stream function theory is used.

Another advantage in considering Eq. (7) is in the clear realization of whether the wave force is dominated by water acceleration or velocity effects. If $\hat{\phi}$ is 1.0, clearly the force is acceleration dependent. If it is 0.0 it is velocity (drag) dependent. Further discussion on this point can be seen in (7).

RESULTS

The SRC.03 could not be towed, so no C_{ds} values are presented for it. The results of circumferential measurement of the various cylinders are given in Table 2.

Table 2. Effective diameter coefficients for the various cylinders from circumferential measurements and sand sizes.

Designation	ε/D	δ
SMC	0	1.00
SRC.02	.023	1.046
SRC.03	.032	1.064
SP1-55	.037	1.074
SP1-140	small	1.00
SP1-190	0	1.00

The SP1-190 cylinder was so smooth that it was not tested. The SP1-140 only had a few very small anemones and a few other crusty organisms. The SP1-55 cylinder had a large number of acorn barnacles attached and one tintinnabulum balanus with average heights of 0.34 inches and a standard deviation of .23 inches. However, the average of several circumferential measurements yielded the results given in Table 2.

Steady tow test results for the SMC, SRC.02, SP1-140 and SP1-55 cylinders are shown in Figs. 4 through 7. There is some obvious scatter in Fig. 5, the true source of which is unknown. Some of it is probably due to small amplitude vibrations of the tow carriage, modifying the wake separation points to some degree. Figure 5 also indicates that the C_{ds} values may be influenced about 2.9% or less because of limited water space above the cylinder (surface effects). This magnitude of difference was later verified with additional testing. Figure 6 shows that the SP1-140 cylinder had a roughness between that of the SMC and the SRC.02. Figure 7 shows that the roughness of the SP1-55 cylinder did not change appreciably between the live, after, and dried conditions. In addition, its roughness appeared to be about equal to that for the SRC.02.

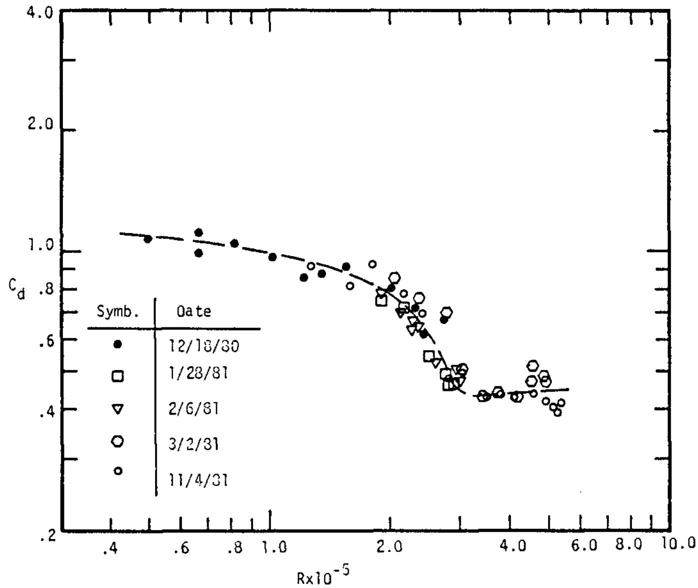

Fig. 4 Steady state tow C_{ds} for SMC.

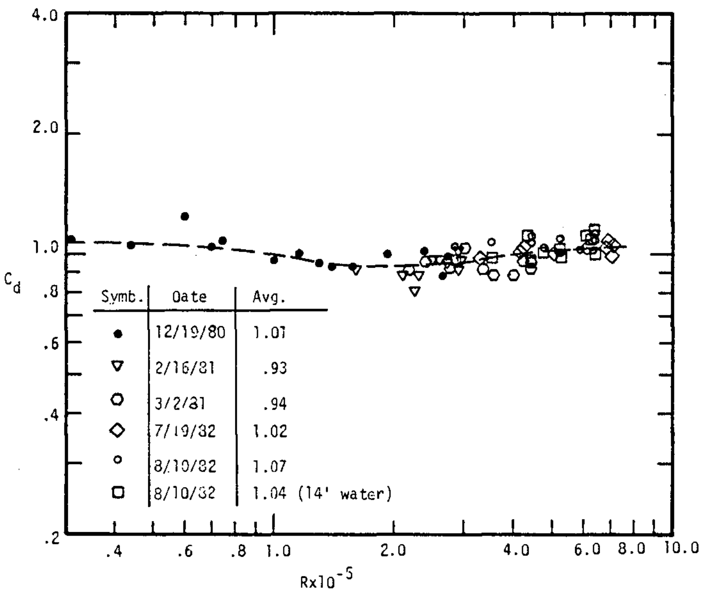

Fig. 5 Steady state tow C_{ds} for SRC.02.

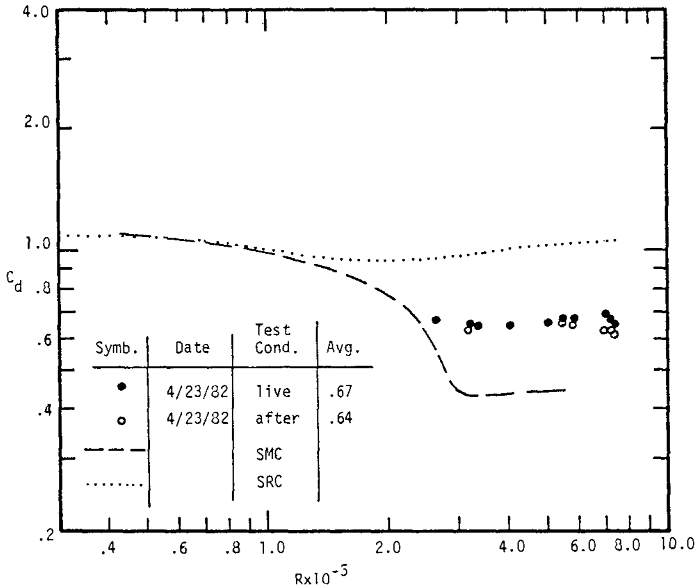

Fig. 6 Steady state tow C_{ds} for SP1-140.

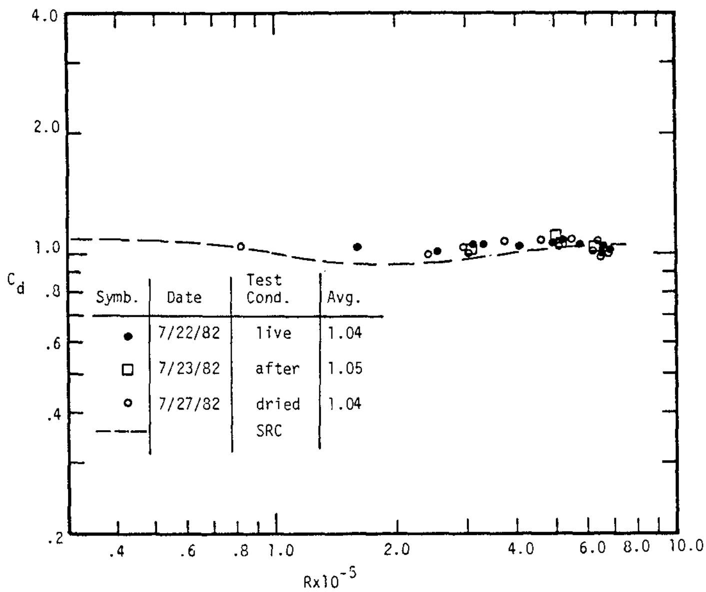

Fig. 7 Steady state tow C_{ds} for SP1-55.

Figure 8 shows the results for C_d from periodic waves for the SMC, SRC.02 and SRC.03 cylinders for 15<K<25. All results fall below those for the results from (8) for oscillatory flow (Ω = o), for K = 20. The results for the SMC have a lot of scatter around R = 1.8×10^5, the true source of which is not yet known.

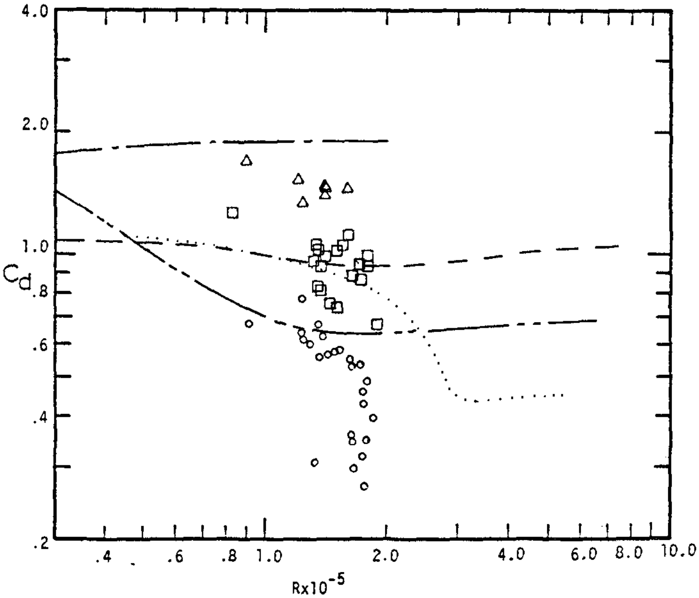

Fig. 8 Drag coefficients in steady tow and wavs for: ——— - ——Sarpkaya (8), ε/D = .02, K = 20;——— - - ——Sarpkaya (8), smooth, K = 20;—— —— ——C_{ds}, SRC.02; ········ C_{ds}, smooth; △ SRC.03, 15 < K < 25; □ SRC.02, 15 < K < 25; ○ smooth, 15 < K < 25.

Figure 9 shows the same results for the SP1-140 and SP1-55 cylinders. Figures 10 and 11 are the counterparts of 9 and 10, only for C_m. These results show very approximately that the SP1-55 cylinder has an equivalent $\varepsilon/D \simeq .03$ and the SP1-140 is somewhere between the smooth condition and $\varepsilon/D \simeq .02$.

The data for the SRC.02, SRC.03, and the SP1-55 were also processed according to Eqs. 6 and 7 using the δ values indicated in Table 2. The results are plotted in Figs. 12 and 13. Figure 12 fairly clearly shows how $C\mu$ increases with roughness in the range of $4 < K < 15$ In addition, the C_{ds} values for SP1-55 and the SRC.02 are plotted at high K in Fig. 12. In the range $15 < K < 25$ the differences in $C\mu$ are less clear. The figure indicates that the experimental $C\mu$ values may well merge with the C_{ds} values at high K and that $C_{ds} \simeq 1.0$ for both $\varepsilon/D \simeq .03$ and $\varepsilon/D \simeq .02$ providing the proper δ is used. This figure may have considerable importance because it implies the $C\mu$ values for the region of $25 < K < 200$, which includes the full scale values of K for ocean platforms.

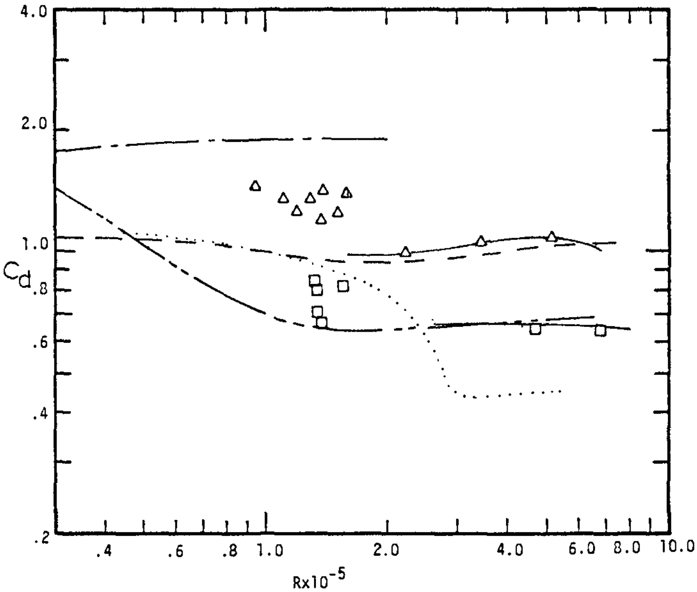

Fig. 9 Drag coefficients in steady tow and waves for: ——— - ——— Sarpkaya (8), $\varepsilon/D = .02$, $K = 20$; ——— - - ——— Sarpkaya (8), smooth, $K = 20$; — ——— C_{ds}, SRC.02; —△— C_{ds}, SP1-55; ——□—— C_{ds}, SP1-140; △ SP1-55, $15 < K < 25$; □ SP1-140, $15 < K < 25$.

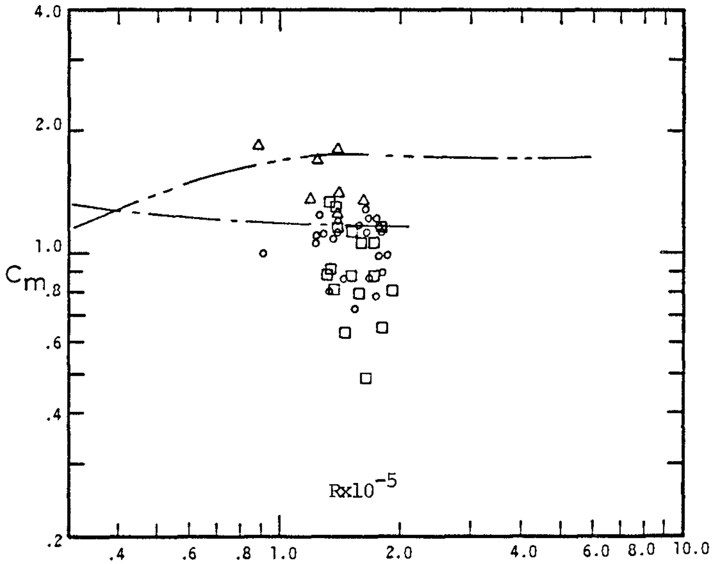

Fig. 10 Inertia coefficients for:——- ——— Sarpkaya (8), ε/D =.02, K = 20;——-- ——— Sarpkaya (8), smooth, K = 20; △ SRC.03, 15 < K < 25; □ SRC.02; 15 < K < 25; ○ smooth, 15 < K < 25.

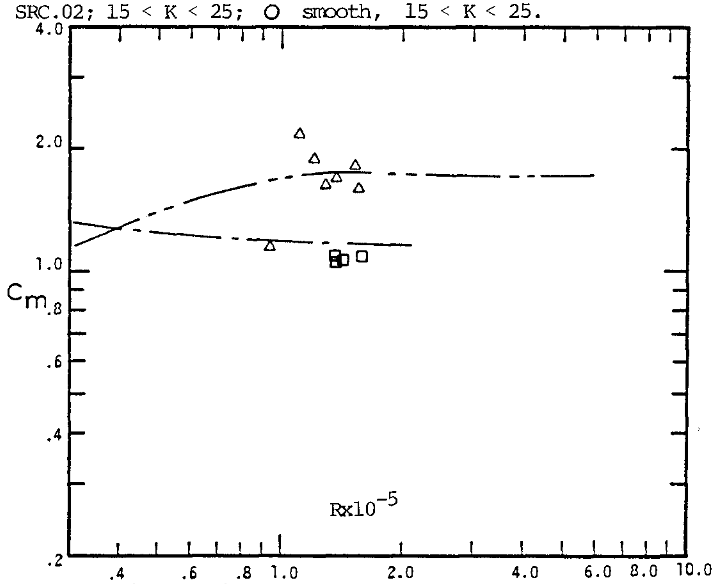

Fig. 11 Inertia coefficients in waves for:——- ——— Sarpkaya (8), ε/D = .02, K = 20;———-- ——— Sarpkaya (8), smooth, K = 20; △ SP1-55, 15 < K < 25; □ SP1-140, 15 < K < 25.

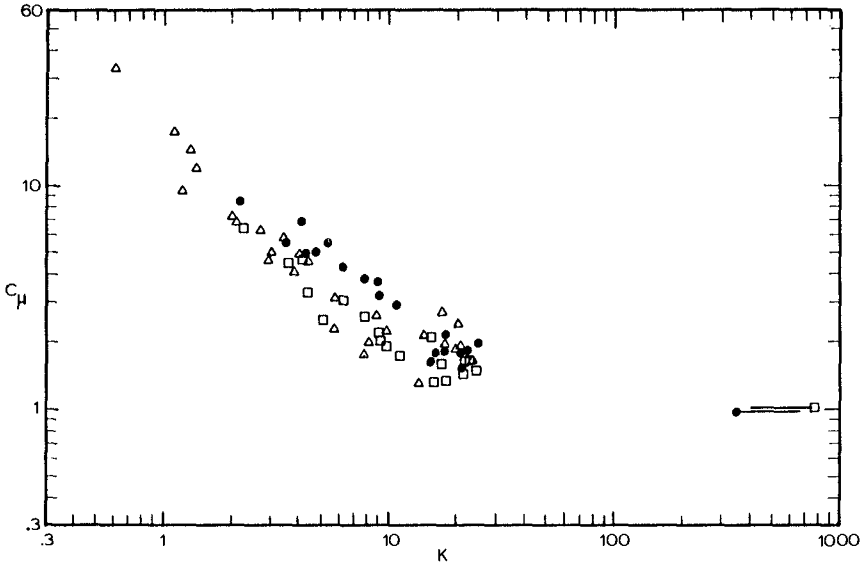

Fig. 12 Maximum force coefficient, horizontal cylinder in waves for: ● SP1-55; △ SRC.03; □ SRC.02; ——□ C_{ds}, SRC.02; ●—— C_{ds}, SP1-55.

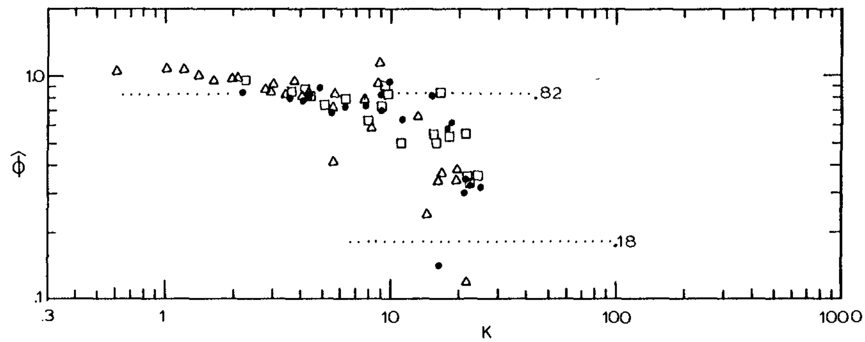

Fig. 13 Phase shift, horizontal cylinder in waves for: ● SP1-55; △ SRC.02; □ SRC.02.

The phase shift results are plotted in Fig. 13. Not surprisingly, scatter is more prevalent in the range $6<K<20$. It is clear that as K increases, the maximum force on the cylinder becomes more velocity (drag) dependent. What is not clear, surprisingly, is that the rougher cylinders are not more drag dependent in the range $10<K<20$. More data are required to determine relationships on a statistical basis for so much scatter. However, at $K = 25$ the few data available indicate that the SP1-55 is more drag dominated than the SRC.02; furthermore, $\hat{\phi}$ is about the same for SP1-55 and the SRC.03. Perhaps the differences in roughness in this study do not have an important influence on the value of $\hat{\phi}$ because as K increases due to an increase in ε/D, $\hat{\phi}$ tends to increase because K becomes smaller ($K=u_\mu T/D\delta$); but, as the surface roughness increases, the flow should become more drag dependent, tending to make $\hat{\phi}$ decrease. These opposing trends tend to compensate.

CONCLUSIONS

Within the range of tests herein the soft fuzzy growths that covered the barnacle-type growths neither appreciably increased nor decreased the drag or inertia coefficients.

The effective roughness of the SP1-55 cylinder was about $\varepsilon/D \approx .03$ and the effective diameter coefficient was about $\delta \approx 1.07$.

For drag dominated flow and high K values, the maximum force coefficient should approach the value of C_{ds}. Furthermore, within these tests, $C_{ds} \approx 1.0$ for all rough cylinders providing appropriate values of δ are used, which can be determined from circumferential measurements.

ACKNOWLEDGEMENTS

The placement and retrieval of the cylinder was done by Chevron USA. Support for the tests and the transfer coefficient analysis was from the American Petroleum Institute. The $C\mu$ and ϕ analysis support was provided partially by the OSU Sea Grant Program, Grant No. NA 81AA-D-00086, and partially by the National Science Foundation, Grant No. CEE-8310732. The author gratefully acknowledges the support from each of these organizations.

REFERENCES

1. Hudspeth, R.T., Jones, D., and J.H. Nath, "Design of Hinged Wave makers for Random Waves," International Conference on Coastal Engineering, Hamburg, Germany, August 1978.

2. Nath, J.H. and K. Kobune, "Periodic Theory Velocity Prediction in Random Waves," International Conference on Coastal Engineering, Hamburg, Germany, August 1978.

3. Nath, J.H., "Drift Speed of Buoys in Waves," (with appendix by M.S. Longuet-Higgins), International Conference on Coastal Engineering, Hamburg, Germany, August 1978.

4. Nath, J.H., "Hydrodynamic Coefficients for Macro-Roughness," Proceedings of Offshore Technology Conference, OTS 3989, May 1981.

5. Nath, J.H., "Heavily Roughened Horizontal Cylinders in Waves," Proceedings of BOSS82, Massachusetts Institute of Technology, August 1982.

6. Nath, J.H., "Hydrodynamic Coefficients for Cylinders Roughened by Marine Growths from the Gulf of Mexico," Final Report to the American Petroleum Institute, Ocean Engineering Program, Department of Civil Engineering, Oregon State University, January 1983.

7. Nath, J.H., et.al., "Laboratory Wave Forces on Vertical Cylinders," Proceedings of the Ocean Structural Dynamics Symposium, Oregon State University, September 1984.

8. Sarpkaya, T., and M. Isaacson, "Mechanics of Wave Forces on Offshore Structures," Van Nostrand-Reinhold, 1981.

9. Sarpkaya, T., Discussion of Ref. 10, Journal of Waterway, Port, Coastal and Ocean Division of ASCE, February 1984.

10. Stansby, P.K., Bullock, G.N., and I. Short, "Quasi-2-D Forces on a Vertical Cylinder in Waves," Journal of Waterway, Port, Coastal and Ocean Division, ASCE, February, 1983.

11. Teng, C.C., and J.H. Nath, "Wave and Current Forces on Cylinders," Proceedings of the Ocean Structural Dynamics Symposium, Oregon State University, September 1984.